



Mist cannon trucks can exacerbate the formation of water-soluble organic aerosol and PM_{2.5} pollution in the road environment

Yu Xu¹, Xin-Ni Dong², Chen He³, Dai-She Wu⁴, Hong-Wei Xiao¹, and Hua-Yun Xiao¹

¹School of Environmental Science and Engineering, Shanghai Jiao Tong University, Shanghai 200240, China

²Jiangxi Province Science and Technology Information Institute, Nanchang 330000, China

³State Key Laboratory of Heavy Oil Processing, China University of Petroleum, Beijing 102249, China

⁴School of Resource, Environmental and Chemical Engineering, Nanchang University, Nanchang 330031, China

Correspondence: Hua-Yun Xiao (xiaohuayun@sjtu.edu.cn)

Received: 27 October 2022 – Discussion started: 16 January 2023

Revised: 28 April 2023 – Accepted: 22 May 2023 – Published: 20 June 2023

Abstract. Mist cannon trucks have been widely applied in megacities in China to reduce the road dust, since they are considered to be more water saving and efficient than the traditional sprinkling trucks. However, their effect on the formation of water-soluble organic compounds and the pollution control of fine particles (PM_{2.5}) remains unknown. We characterized the variations of chemical compositions in PM_{2.5} collected on the road sides during the simulated operations of mist cannon truck and traditional sprinkling truck via Fourier transform ion cyclotron resonance mass spectrometry and ion chromatography. The mass concentrations of water-soluble organic carbon in PM_{2.5} showed a significant increase (62 %–70 %) after air spraying. Furthermore, we found that water-soluble organic compounds, particularly organic nitrates, increased significantly via the interactions of reactive gas-phase organics, atmospheric oxidants and aerosol liquid water after air spraying, although the air spraying had a better effect on suppressing road dust than the ground aspersion. Moreover, the formation of PM_{2.5} on the road segment where the mist cannon truck passed by was promoted, with an increase of up to 13 % in mass concentration after 25–35 min, on average. Thus, the application of mist cannon trucks potentially worsens the road atmospheric environment through the increase in PM_{2.5} levels and the production of a large number of water-soluble organic compounds in PM_{2.5}. The overall results provide not only valuable insights to the formation processes of water-soluble organic compounds associated with aerosol liquid water in the road environment but also management strategies to regulate the operation of mist cannon trucks in China.

1 Introduction

Over the past decade, the demand for effective road dust control has grown dramatically due to the upgraded environmental protection policies. Traditionally, the sprinkling trucks with the ground aspersion work well for vehicle-generated road dust. The newly developed mist cannon trucks are able to spray water mist up to 120 m away and 100 m high, with a droplet diameter of as small as 5 μm. They are considered to be more water saving and efficient than the traditional sprinkling trucks (the ground aspersion), although the rele-

vant argumentation work is rarely systematically studied. In recent years, the mist cannon trucks have been widely utilized by the local environmental bureau to achieve the target of strict emission control in megacities in China (Wang et al., 2022). Traffic-related emissions contribute a huge amount of volatile organic compounds (VOCs), nitrogen oxides (NO_x), ammonia (NH₃) and fine particles (PM_{2.5}) to the urban atmosphere, which exerts adverse impacts on human health and climate change (Yang et al., 2022; Deng et al., 2020). However, no study has investigated whether and how the water

mist sprayed by mist cannon trucks affects the road atmospheric environment.

The mist cannon trucks can spray a large amount of fine water mist in a short time; hence, the air humidity of a local road environment where the mist cannon truck passed by will increase sharply. Aerosol liquid water (ALW) exists in the condensed phase as a function of gas and particle chemical composition, particle concentration, temperature (T) and relative humidity (RH) (Xu et al., 2020b; Nguyen et al., 2015). Thus, an increase in RH can promote the rise in ALW concentration (Guo et al., 2015). It is well documented that ALW plays an important role in the formation of secondary organic aerosol (SOA) via the partitioning of gas-phase water-soluble organics to the particle phase and subsequent aqueous-phase reactions (Sareen et al., 2017; Carlton and Turpin, 2013). The severe haze episodes in Beijing can even be partly attributed to the interactions between ALW (or high RH) and aerosol organic components (W. Li et al., 2019; Wang et al., 2021). In particular, 40%–80% of fossil-fuel-derived primary organic aerosols were found to be water soluble (Qiu et al., 2019). However, there are large knowledge gaps in our current understanding on ALW-related organic compound formation in the road environment with mist cannon truck operation.

Although few studies have systematically evaluated the ability of mist cannon trucks to remove road dust, it is easy to understand that the tiny water droplets generated by the mist cannon system can indeed capture coarse particles (i.e., dropping dust to the ground) more effectively than the water column sprayed by the traditional sprinkling truck. However, fine particles ($PM_{2.5}$) are commonly regarded as a major threat to urban atmospheric environment and human health (Yue et al., 2020). Thus, assessing the impact of mist cannon truck operation on road $PM_{2.5}$ pollution is of great significance for guiding future environmental protection initiatives.

In this study, we simulated the operation scenes of mist cannon trucks and traditional sprinkling trucks on the sides of the urban road (Nanchang, eastern China). We collected ambient $PM_{2.5}$ samples in these scenes. The molecular compositions of water-soluble organic matter (WSOM) in the collected samples were resolved using ultrahigh-resolution Fourier transform ion cyclotron resonance mass spectrometry (FT-ICR MS). Moreover, we also presented the measurement of other chemical components (e.g., water-soluble ions) in $PM_{2.5}$ samples and the predicted ALW concentration. The concentrations of $PM_{2.5}$ were also monitored on the road segment where the mist cannon truck passed by. The overall results will shed light on the impact of spraying water mist by mist cannon trucks on the formation of water-soluble organic compounds and its implications for $PM_{2.5}$ pollution control in the urban road environment for the first time.

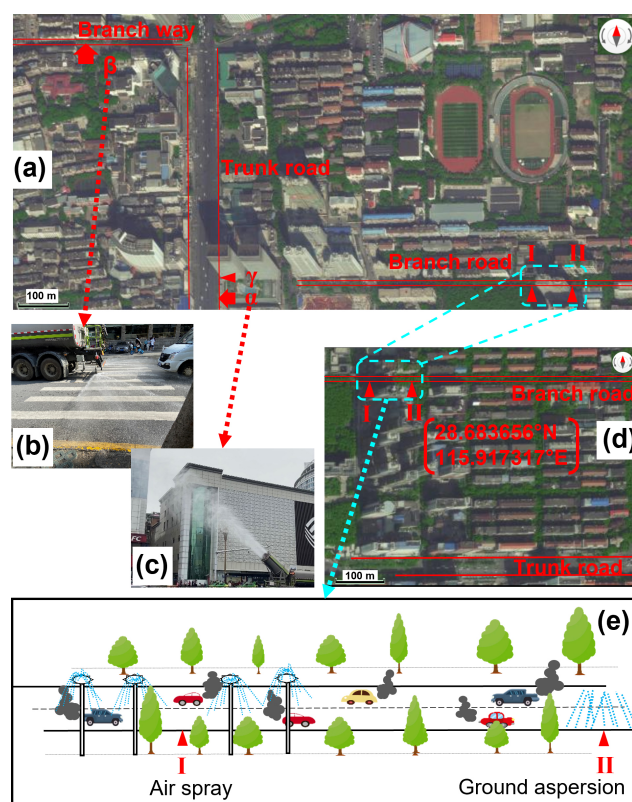


Figure 1. Map (Baidu, China) showing (a) the study area. The symbol of “ γ ” indicates the location where $PM_{2.5}$ mass concentration was monitored. The symbols of “ α ” and “ β ” refer to the locations where (b) the mist cannon truck photograph and (c) the traditional sprinkling truck photograph were taken, respectively. The symbol of “I” indicates that (d) the sampling was conducted on the air spray road segment or no water spray road segment (I). The symbol of “II” indicates that (d) the sampling was conducted on the ground aspersion road segment or no water spray road segment (II). Panel (e) shows the conceptual diagram of the sampling campaign.

2 Materials and methods

2.1 Study site and sample collection

A branch road (provincial capital north second road) located in the center of Nanchang (eastern China) was selected as the study area (Fig. 1a). This area is characterized by heavy traffic and high population density. There are no typical pollution sources, such as factories and garbage treatment plants, within 30 km of the study area. The trees on both sides of the road are very tall and lush (Fig. 1a), which makes the atmosphere in this road environment relatively stable. The dominant tree species in this area is camphor trees (*Cinnamomum camphora*). Thus, the region is expected to be influenced by both anthropogenic (e.g., vehicle exhausts) and biogenic VOCs.

Two sampling points (a distance of approximately 70 m) on the road side were selected, which were affected by air

spray and ground aspersion, respectively (Fig. 1b–e). The air spraying at a height of 8 m above the ground was to simulate the water mist sprayed by the mist cannon truck. In contrast, the ground aspersion with a height of 0.4 m above the ground was designed to simulate the operation of a traditional sprinkling truck. The residence time of the fine water mist sprayed by the mist cannon truck in the air is assumed to be several minutes to tens of minutes, which mainly depends on the ambient temperature, RH and wind speed. As mentioned above, the lush trees on both sides of the road cause the atmosphere in the road environment to be relatively stable. Moreover, we found that each simulated air spray can maintain a high level of RH for several minutes (about 4–8 min). Thus, the frequency of spraying water (Milli-Q water, 18.2 M Ω cm) was set to 1 min, spraying every 8 min in this study. This spraying operation can prevent the resuspension of road dust as much as possible. The spraying was controlled by intelligent timing irrigation equipment (Nadster, China). The diameter of the pores in the nozzle for air spraying is less than 0.8 mm, while that in the nozzle for ground aspersion is approximately 6 mm.

PM_{2.5} samples were collected onto prebaked (500 °C for ~10 h) quartz fiber filters (Pallflex, Pall Corporation, USA) using a high-volume air sampler (Series 2031, Laoying, China). Sampling at the above-mentioned two sites was simultaneously performed from 23 to 26 March 2021. The duration of each aerosol sampling was approximately 4 h (09:00–13:00 LT) every day. We observed that the traffic flow on 25 March was higher than that on other days. The weather during the sampling periods from 23 to 26 March was cloudy to sunny, sunny, sunny and showers (only one short precipitation event in the sampling period), respectively. The average ambient *T* was approximately 21 °C. The average ambient RH in those periods (23–25 March) ranged between 50 % and 60 %. The average RH can reach 84 %–87 % after air spraying. On 26 March, the average ambient RH was as high as 80 % during the period of 09:00–13:00. Thus, the water spraying operation was stopped when the samples were collected on 26 March. All samples were stored at –28 °C prior to the analysis. In addition, the mass concentrations of PM_{2.5} were measured online (Thermo Scientific 5030i, USA) from July to August 2021 near the trunk road where the mist cannon truck was frequently operated (Fig. 1a). Typically, the mist cannon truck was operated back and forth on specific road sections to prevent the resuspension of dust. Thus, the PM_{2.5} online monitoring was performed after the misting cannon truck passed through the monitoring point several times. Specifically, PM_{2.5} concentrations near the road (81 road, Nanchang) were recorded at 5 min intervals from 10 min before to 50 min after the mist cannon truck passed by.

2.2 Chemical analysis

A portion of each filter sample was ultrasonically extracted with Milli-Q water (MQW). WSOM in the extracting solution was further extracted using the previously reported solid-phase extraction (SPE) method (Dittmar et al., 2008; Qiao et al., 2020; Xie et al., 2020). Briefly, the cartridge (PPL, 0.5 g, Agilent) was rinsed with 18 mL of methanol (LC-MS grade, Thermo Fisher) and 18 mL of HCl solution (pH = 2) in turn. Subsequently, the extracts with acidity adjusting (pH = 2) were injected into a cartridge. Acidified MQW (18 mL) and normal MQW (6 mL) were added in turn to remove the salt and chloride ion trapped in the cartridge. After drying under a stream of N₂, trapped OM was eluted using 15 mL of methanol. The eluted solution was concentrated to 4 mL and then preserved at –28 °C until analysis. The molecular compositions of WSOM in PM_{2.5} samples were determined using a Bruker apex-ultra Fourier transform ion cyclotron resonance mass spectrometry (FT-ICR MS) (Bruker, Germany) coupled to an Apollo II electrospray ionization (ESI) (He et al., 2020). The samples were injected into the ionization source at 250 μ L h^{–1} through a syringe pump. The instrument was operated in the negative-ion mode. Continuous scans totaling 128 were acquired in each analysis to increase the signal-to-noise ratio of the mass spectrum. Blank was analyzed with the same procedure. Detailed methodologies and data quality control have been described elsewhere (He et al., 2019, 2020).

Another filter cut was ultrasonically extracted with MQW for the determination of water-soluble organic carbon (WSOC), water-soluble total nitrogen (WSTN) and inorganic ions. The mass concentrations of WSOC and WSTN in samples were measured with a total organic carbon/total nitrogen analyzer (Elementar vario, Germany) (Xu et al., 2019). The mass concentration of WSOC was converted to that of WSOM using a conversion factor of 1.8 (Müller et al., 2017; Finessi et al., 2012; Yttri et al., 2007; Simon et al., 2011). The mass concentrations of water-soluble inorganic ions, such as SO₄^{2–}, NO₃[–], NH₄⁺ and K⁺, were measured using an ion chromatography system (Dionex, Thermo, USA) (Xu et al., 2020a, 2022). The mass concentration of water-soluble organic nitrogen (WSON) was calculated as the difference in the concentrations between WSTN and inorganic nitrogen (i.e., NO₃[–]_N + NO₂[–]_N + NH₄⁺_N) (Xu et al., 2020b). Ambient *T* and RH were measured using a temperature and humidity monitor (CEM 9880M, China).

2.3 Compound categorization and ALW prediction

The molecular formulas assigned from FT-ICR MS were classified into four main compound groups in this study. These identified groups include CHO (containing only C, H and O), CHON (containing C, H, O and N), CHOS (containing C, H, O and S), and CHONS (containing C, H, N, O and S; Song et al., 2018). The double-bond equivalent (DBE)

was calculated to describe the unsaturation degree of the organic compounds (see details in Sect. S1 in the Supplement; Schmidt et al., 2017; Qiao et al., 2020). The modified aromaticity index (AI_{mod}) was calculated to reflect the aromaticity of organic molecules (see details in Sect. S1 in the Supplement) (Schmidt et al., 2017; Koch and Dittmar, 2006). The carbon oxidation state (OSc) was used to indicate the evolving composition of aerosol organics that underwent oxidation processes (Kroll et al., 2011). The details of the OSc calculation are shown in Sect. S1 in the Supplement. According to the oxygen-to-carbon (O/C) and hydrogen-to-carbon (H/C) elemental ratios, the identified molecular formulas were further classified into five compound categories, including unsaturated aliphatic-like (UA), highly unsaturated-like (HU), highly aromatic-like (HA), polycyclic aromatic-like (PA), and saturated-like (Sa) molecules (Su et al., 2021). These classified compound categories were visualized in the van Krevelen diagram (see details in Sect. S1).

The thermodynamic model ISORROPIA II was applied to calculate the mass concentrations of ALW driven by inorganic components (Guo et al., 2015; Tan et al., 2017; Xu et al., 2022). The model predicts the inorganic ALW based on the mass concentrations of inorganic species, RH and T (see details in Sect. S2). Particle hygroscopicity is also influenced by organics in aerosol particles (Sareen et al., 2013; Cruz and Pandis, 2000). The impact of organic fraction on aerosol water is complex and depends on the composition of organic matter (Nguyen et al., 2016). In this study, the mass concentration of water associated with aerosol organic fraction was predicted according to the previously reported method (see details in Sect. S2; Nguyen et al., 2015, 2016).

3 Results and discussion

3.1 Chemical characteristics of $PM_{2.5}$ in different road segments

Figure 2 compares the differences in the chemical composition of $PM_{2.5}$ collected in the air spray road segment and ground aspersion road segment. The mass fraction of WSOM was the highest regardless of the weather and road section where the samples were collected, which accounted for 30%–40% of the total water-soluble components (Fig. 2a–d). From 23 to 25 March, the mass concentrations and fractions of WSOM (WSOC) were higher on the air spray road segment than on the ground aspersion road segment. For the case without water spray treatment (as a reference group), the chemical compositions of $PM_{2.5}$ samples collected from those two adjacent road segments only showed small differences in concentration (Fig. 2d, h, i). It suggested that the impact of background $PM_{2.5}$ or the meteorological factor on $PM_{2.5}$ composition or level was similar between these two study sites. Obviously, the variations in the mass concentrations and fractions of WSOM from the air spray road segment to the ground aspersion road segment can be attributed

to the differences in water-soluble SOA yield or formation pathway caused by different water spray treatments.

The mass concentrations of ALW, WSOC and WSON tended to decrease from the air spray road segment to the ground aspersion road segment (Fig. 2e–g). Moreover, linear regression analysis showed that the mass concentrations of ALW ($n = 8$) were significantly positively ($P < 0.01$) correlated with those of WSOC and WSON, with R^2 values of 0.84 and 0.75, respectively. The results were consistent with those obtained by previous studies conducted in an agricultural area in Italy (Hodas et al., 2014) and a suburban forest site in Tokyo (Xu et al., 2020b). Moreover, these studies by Hodas et al. (2014) and Xu et al. (2020b) suggested that the ALW dependence of reactive gas uptake and subsequent aqueous reactions significantly contributed the production of WSOC and WSON. Thus, the increase in ALW concentration after air spraying can promote the formation of water-soluble organic compounds in $PM_{2.5}$ in the road environment.

Nitrate and sulfate were the most abundant inorganic components (Fig. 2a–d), which have been identified as typical factors controlling ALW (Hodas et al., 2014). From the air spray road segment to the ground aspersion road segment, the decrease in nitrate concentration was more significant than that in sulfate concentration (Fig. 2i–k). Moreover, the concentration of nitrate significantly correlated with that of ALW ($P < 0.01$, $R^2 = 0.7$). In contrast, the sulfate did not show a strong correlation with ALW ($R^2 = 0.3$). As we know, the gas-phase oxidation of NO_2 by hydroxyl radical ($\cdot OH$) to form nitric acid (HNO_3) is an important pathway for the formation of daytime nitrate aerosol (Fu et al., 2020; Chen et al., 2020). Hydroxyl radical can be rapidly produced by O_3 photolysis under conditions with abundant water vapor and sunlight (as in this study) (Li et al., 2022), which is undoubtedly beneficial to the production of HNO_3 . Thus, in the region with large NO_x and ammonia emissions (originating from vehicle exhausts; Yang et al., 2022), the formation of daytime nitrate aerosol could be promoted by enhanced RH (24%–43% increase) after air spraying. This is also partly supported by the thermodynamics of ammonium nitrate formation (Mozurkewich, 1993; Hodas et al., 2014). Additionally, it has been suggested that the formation of nitrate and ALW is mutually reinforcing (Chen et al., 2022). Thus, the increase in ALW concentration after air spraying was mainly driven by RH and locally (traffic emissions) formed nitrate aerosol.

Interestingly, Ca^{2+} and Mg^{2+} showed a significant increase in concentration from the air spray road segment to the ground aspersion road segment (Fig. 2i–k), which was contrary to the case of other components (e.g., WSOC, ALW and nitrate). In addition, during 26 March without water spray treatment, the differences in both Ca^{2+} and Mg^{2+} concentrations between those two adjacent road segments were almost negligible (Fig. 2l). It is well known that Ca^{2+} and Mg^{2+} are typical crustal materials and are mainly enriched in at-

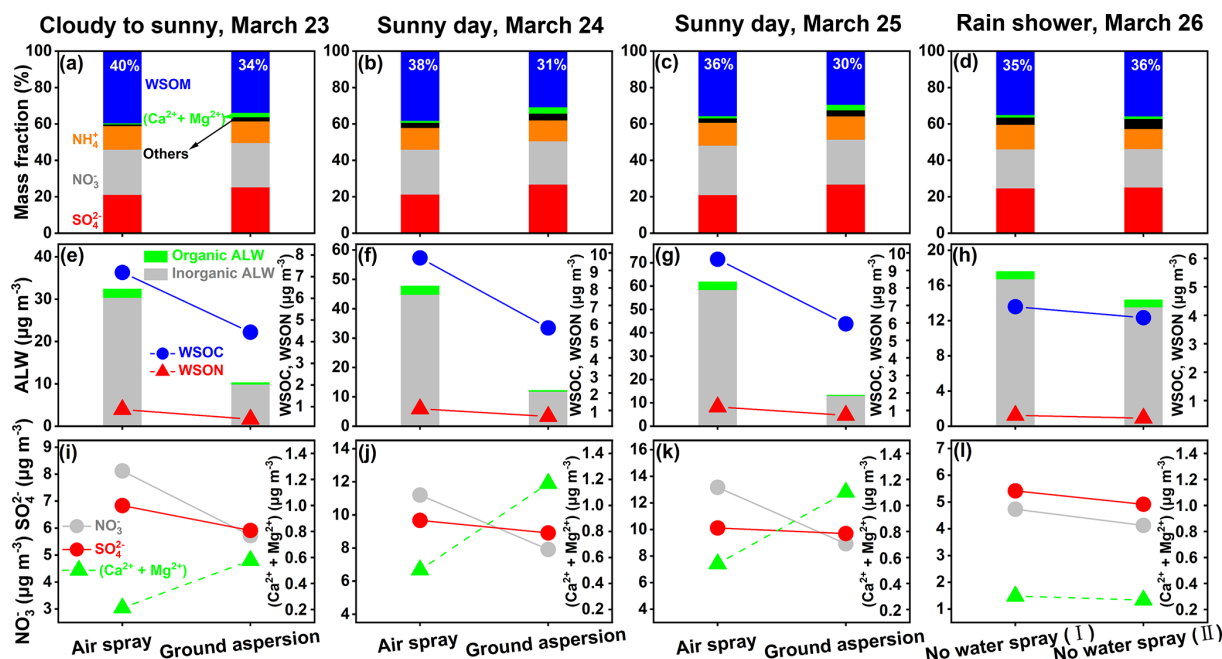


Figure 2. The mass fractions of chemical components in $\text{PM}_{2.5}$: (a–c) air spray vs. ground aspersions and (d) no water spray (I) vs. no water spray (II). The mass concentrations of ALW, WSOC and WSON in $\text{PM}_{2.5}$: (e–g) air spray vs. ground aspersions and (h) no water spray (I) vs. no water spray (II). The mass concentrations of NO_3^- and SO_4^{2-} , as well as the sum of Ca^{2+} and Mg^{2+} concentrations in $\text{PM}_{2.5}$: (i–k) air spray vs. ground aspersions and (l) no water spray (I) vs. no water spray (II).

atmospheric coarse particles (Chen and Chen, 2008). Thus, a decrease in Ca^{2+} and Mg^{2+} concentrations after air spraying implied that the water mist sprayed by mist cannon trucks had a better effect on suppressing road dust than the ground aspersions by traditional sprinkling trucks.

3.2 Molecular characteristics of water-soluble organic compounds

Thousands of molecular formulas (5966–8102) were observed in WSOM in $\text{PM}_{2.5}$ collected from the road environment (Table 1). The CHO molecular formulas (1089–2037) accounted for 20%–25% in all molecular formulas. Further, CHO compounds were classified according to the number of oxygen atoms in their molecules. The subgroups ranged from O_2 to O_{15} (Fig. 3). The number and intensity of dominated O_5 – O_{10} subgroups accounted for 72%–85% and 71%–86% of the total compounds, respectively; moreover, these percentages were higher than the results reported for aerosols in Beijing (Xie et al., 2020). The average H/C and O/C ratios of CHO compounds varied from 1.08 to 1.24 and from 0.42 to 0.49, respectively (Table S1). The average O/C ratios were higher than the value (0.33 ± 0.11) obtained from urban aerosols (Beijing, China), while the H/C ratios showed relatively small differences between our results and observation results in Beijing (1.14 ± 0.37 ; Xie et al., 2020). In addition, another study performed in Beijing showed that the average O/C and H/C ratios of organic aerosols were in the range

of 0.47–0.53 and 1.52–1.63, respectively (Hu et al., 2017). These dissimilarities might be attributed to the fact that the sources of urban aerosols are more complex than those of aerosols collected from road environments.

The average H/C and O/C ratios of CHON compounds ranged from 1.05 to 1.21 and 0.42 to 0.51, respectively (Table S1). The H/C ratio ranges of CHON compounds in this study overlapped with those measured in previous studies (Su et al., 2021; Xie et al., 2020). However, the O/C ratios of CHON compounds were relatively higher in road-derived aerosols than in aerosols (0.36 ± 0.12) or snow (0.32 – 0.37) collected in urban areas (building roof; Su et al., 2021; Xie et al., 2020). This difference might be associated with the influence of source strength (e.g., vehicle exhausts) and atmospheric oxidation capacity. The number of CHON formulas (1501–2685) was much higher than that of CHO formulas (Table 1). The assigned CHON formulas were further divided into CHON_1 (N_1O_2 – N_1O_{16}), CHON_2 (N_2O_2 – N_2O_{13}) and CHON_3 (N_3O_2 – N_3O_{13}) groups (Fig. 3). CHON_1 was found to be the dominant nitrogen-containing species in all samples, which was consistent with previous reports on urban aerosols and snow (Su et al., 2021; Xie et al., 2020). Moreover, the CHON_1 compounds with $\text{O}/\text{N} > 2$ contributed 99.2%–100.0% to total CHON_1 species in all samples. The CHON_2 compounds with $\text{O}/\text{N} > 2$ accounted for 90.2%–100.0% of total CHON_2 species. For the CHON_3 group, the proportion of nitrogen-containing compounds with $\text{O}/\text{N} > 2$ was 53.0%–61.8%. The CHON species with

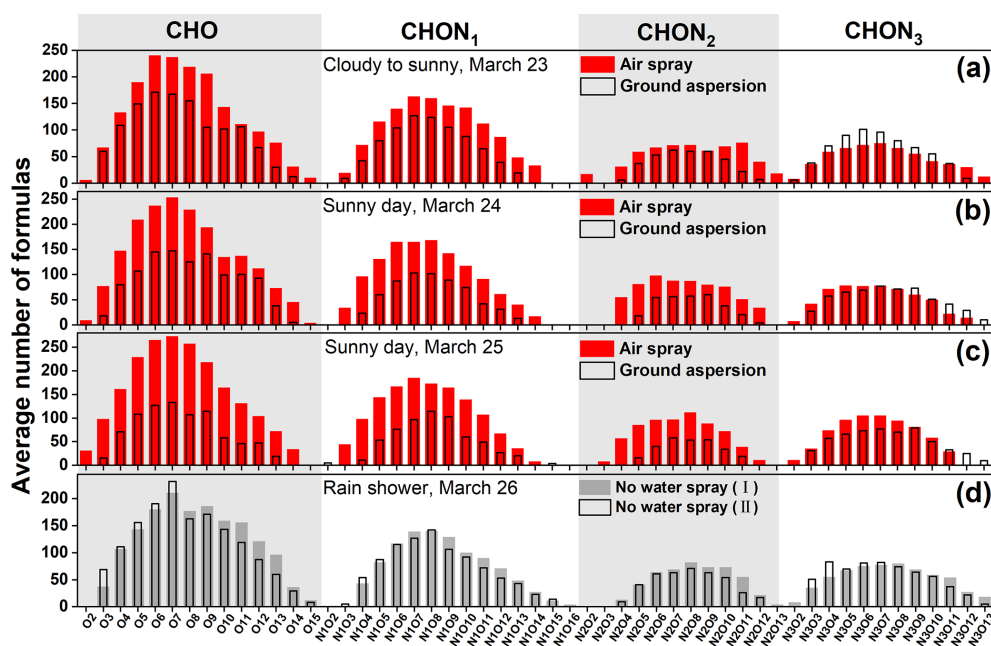


Figure 3. Classification of CHO and CHON species into subgroups according to the number of O atoms in their molecules in WSOM in $\text{PM}_{2.5}$ collected from different cases: (a–c) air spray vs. ground aspersion and (d) no water spray (I) vs. no water spray (II).

Table 1. The number of compounds in different subgroups in different samples and the number fractions of common molecules in the same subgroup in different samples.

Sample type (Date: 23–26 March)	Total	CHO	Common (CHO)	Common fraction (CHO)	CHON	Common (CHON)	Common fraction (CHON)
Air spray (23)	7069	1766	1104	63 %	2375	1308	55 %
Ground aspersion (23)	6166	1233		90 %	1803		73 %
Air spray (24)	7317	1861	990	53 %	2447	1225	50 %
Ground aspersion (24)	6067	1098		90 %	1501		82 %
Air spray (25)	8102	2037	804	39 %	2685	1209	45 %
Ground aspersion (25)	5966	845		95 %	1464		83 %
No water spray (I) (26)	6998	1621	1315	81 %	2120	1579	74 %
No water spray (II) (26)	6990	1539		85 %	1963		80 %

$\text{O}/\text{N} > 2$, which allows an assignment of oxidized-form nitrogen, are preferentially ionized in negative electrospray ionization mode (Lin et al., 2015; Su et al., 2021). Studies on the compositions of organic matter in urban rainwater and aerosols have suggested that numerous CHON compounds contained oxidized nitrogen function groups (e.g., $-\text{ONO}_2$) and that NO_x -related oxidation processes can be responsible for the formation of these CHON compounds (Altieri et al., 2009; Lee et al., 2016). Thus, the CHON compounds with $\text{O}/\text{N} > 2$ in our $\text{PM}_{2.5}$ samples can be assumed to be mostly in an oxidized form (e.g., organic nitrates).

Figure 3 also shows the differences in the number of CHO and CHON species between the air spray road segment and ground aspersion road segment. The abundance of each O_n

subgroup in CHO compounds considerably enhanced after air spraying, especially the subgroups of O_5 – O_{11} . In contrast, the number of CHO species for these two cases without water spray treatment showed a smaller difference (Fig. 3d). In general, the total number of CHO compounds increased significantly after air spraying (Fig. 3 and Table 1). However, there was no significant change for the total number of CHO species between the two cases without water spray treatment. These findings implied that the increased ALW after air spraying can substantially contribute to the formation of CHO compounds with a more oxygenated state.

The number of CHON compounds decreased significantly from the air spray road segment to the ground aspersion road segment, a variation pattern of which was similar to

that of CHO compounds (Fig. 3 and Table 1). Furthermore, the decrease in the number of molecules from the air spray road segment to the ground aspersion road segment was more remarkable for CHON_1 compounds than for CHON_2 compounds. In contrast, the variation in the number of CHON_3 molecules after air spraying was less significant than that of CHON_{1-2} compounds. In addition, an insignificant change in the number of CHO compounds was found in $\text{PM}_{2.5}$ collected in the two road segments without water spray (Fig. 3d). Thus, the increase in the number of nitrogen-containing compounds after air spraying indicated that the interactions among ALW, traffic-derived reactive nitrogen and ambient VOCs may play an important role in organic nitrogen compound formation in $\text{PM}_{2.5}$. This consideration can also be partly supported by the result obtained by Xu et al. (2020b) in a suburban forest in Tokyo, Japan. The authors suggested that ALW is a key promoter for the formation of aerosol WSON through secondary processes associated with atmospheric reactive nitrogen and biogenic VOCs (Xu et al., 2020b). For sulfur-containing compounds, their molecular numbers just showed a relatively small change after air spraying (Fig. S1). This suggested that the impact of ALW on sulfur-containing compound formation was weaker than that of ALW on the formation of CHO and CHON compounds in this road environment.

3.3 CHO and CHON species formed under the influence of increased ALW

The molecular compositions of CHO compounds in $\text{PM}_{2.5}$ in the van Krevelen diagram were scattered across wider ranges in the air spray road segment than in the ground aspersion road segment, particularly on the sunny days (24 and 25 March) (Fig. 4). Moreover, common CHO molecules accounted for 39% (sunny day), –63% (cloudy to sunny day) and 90%–95% of CHO molecules in $\text{PM}_{2.5}$ collected from the air spray and ground aspersion road segments, respectively (Table 1). In contrast, common CHO molecules contributed 81%–85% of CHO molecules in $\text{PM}_{2.5}$ collected from two road segments without water spray (I and II). These results can be explained by the increased molecular diversity caused by ALW-related atmospheric processes. It also implied the importance of photochemical reactions in CHO compound formation. Furthermore, the unique CHO compounds were identified between $\text{PM}_{2.5}$ samples in the air spray road segment (or no water spray road segment, I) and the ground aspersion road segment (or no water spray road segment, II) (Fig. S2). On 23 and 24 March, the newly emerging CHO compounds after air spraying were dominated by unsaturated aliphatic-like and highly unsaturated-like compounds. However, both unsaturated-like species (unsaturated aliphatic-like and highly unsaturated-like) and aromatic-like species (highly aromatic-like and polycyclic aromatic-like) contributed significantly to the newly emerging CHO compounds after air spraying on 25 March when

the ALW and traffic flow were higher than other days (Fig. S2). Obviously, the formation of those unique CHO compounds was closely associated with increased ALW.

Figure 5 shows the OSc values of the identified unique CHO molecules. The OSc values of these CHO molecules were higher than those of primary vehicle exhausts (–2.0 to –1.9) (Aiken et al., 2008). The OSc values of the secondary organic aerosol formed via the reactions of anthropogenic and biogenic VOCs (e.g., isoprene, monoterpene, toluene, alkane and alkene) and oxidants (e.g., O_3 and/or $\bullet\text{OH}$) varied from –1.1 to +1.0 (Kroll et al., 2011; Y. Li et al., 2021), which was within the OSc value ranges of CHO molecules measured in this study. In addition, hydrocarbon-like organic aerosol (HOA), likely linked with primary vehicle exhausts (Sun et al., 2016), only accounted for less than 6% of total unique CHO compounds (Fig. 5). Although it is difficult to classify all CHO molecules in Fig. 5, these identified unique CHO molecules can at least suggest that the water mist from air spraying can promote the formation of CHO compounds and increase their molecular diversity. As mentioned previously, there are dense trees on both sides of the road. Thus, these newly emerging CHO compounds can be largely attributed to secondary processes associated with the oxidation of vehicle exhausts and biogenic VOCs by O_3 and/or $\bullet\text{OH}$. In addition, we also observed increased oligomerization (e.g., methylglyoxal ($\text{C}_3\text{H}_4\text{O}_2$) to form oligomers ($\text{C}_{4-7}\text{H}_{6-10}\text{O}_5$) in particle phase) of CHO compounds after air spraying (Ma et al., 2022), particularly on 25 March, with a high ALW level and a large traffic flow (Fig. S3c). The overall results implied that the water mist sprayed by mist cannon trucks can indeed enhance the abundance and diversity of CHO compounds in $\text{PM}_{2.5}$ via promoting gas-to-particle partitioning of gas-phase oxidation products of VOCs and subsequent aqueous-phase reactions.

For CHON compounds, their molecular compositions were scattered across an increased range in the van Krevelen diagram after air spraying compared to the observations in the ground aspersion case (Fig. S4). This was also indicated by the relatively low proportion of common CHON molecules (45%–55%) in total CHON compounds for the cases with air spraying treatment (Table 1). Moreover, these newly emerging CHON molecules after air spraying showed a high diversity, as shown in Fig. S5. The group of CHON_1 was the dominant nitrogen-containing compound in the identified unique CHON compounds. On 23 and 24 March, the main unique CHON compounds emerged during air spraying were unsaturated aliphatic-like and highly unsaturated-like nitrogen-containing species. The number of highly aromatic-like and polycyclic aromatic-like compounds that newly emerged also increased significantly following increased traffic flow and ALW (25 March). The results suggested that the increase in ALW concentration after air spraying can facilitate the formation of particle-phase nitrogen-containing compounds (Hallquist et al., 2009; Xu et al., 2020b).

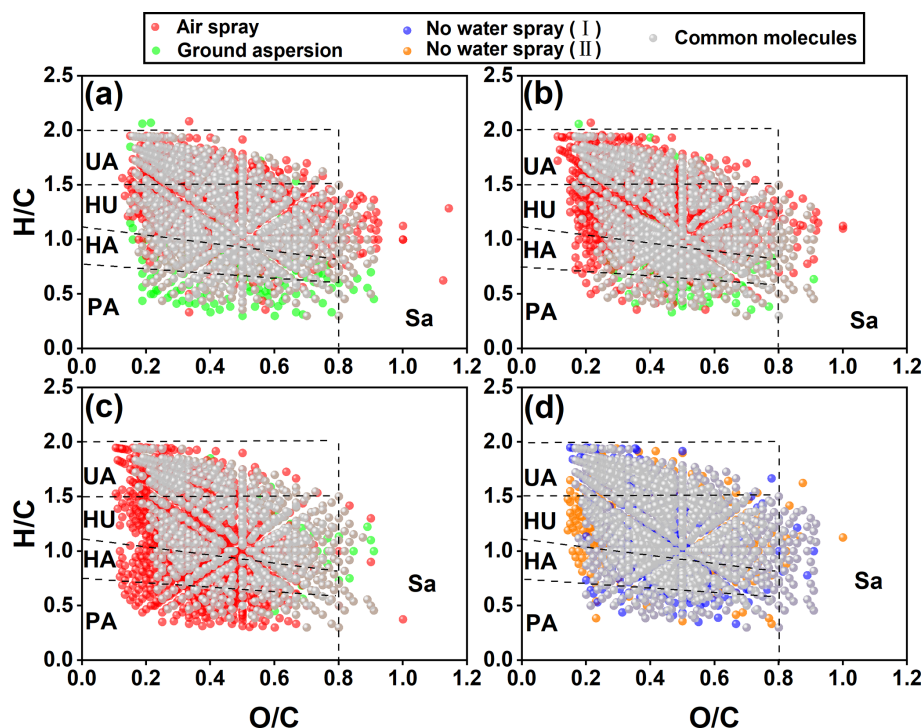


Figure 4. Van Krevelen diagrams of CHO compounds in WSOM in $\text{PM}_{2.5}$ collected from different cases: air spray vs. ground aspersion on (a) 23 March, (b) 24 March and (c) 25 March and two road segments without water spray (I vs. II) on (d) 26 March. The classifications of compounds include unsaturated aliphatic-like (UA), highly unsaturated-like (HU), highly aromatic-like (HA), polycyclic aromatic-like (PA) and saturated-like (Sa) molecules.

Organic nitrates have been supposed to be abundant in our $\text{PM}_{2.5}$ samples collected from the road environment. It is well documented that atmospheric organic nitrates are primary, secondary and tertiary byproducts of reactions among anthropogenic and biogenic VOCs, atmospheric oxidants (e.g., O_3 , $\cdot\text{OH}$, and nitrate radicals), and NO_x (Lee et al., 2016; Yeh and Ziemann, 2014; Su et al., 2021). In addition, numerous organic nitrates are known as semivolatile compounds, which are able to partition between the gas and particle phases when they are oxidized or photolyzed (Bean and Hildebrandt Ruiz, 2016). Recently, an oxidation and hydrolysis mechanism associated with the formation of atmospheric organic nitrates has been proposed to interpret the potential origins or precursors of CHON compounds (Su et al., 2021). In this study, we found that 68%–82% of newly emerging CHON_1 compounds after air spraying can be explained by oxidation (e.g., R_1OH) and product (e.g., R_1ONO_2) pair proposed by Su et al. (2021) (Fig. 6a–c). It indicated that these newly emerging CHON_1 compounds after air spraying were largely derived from the transformation of CHO species under existence of NO_x . A similar pattern was also observed in the newly emerging CHON_2 compounds (Fig. S6). It should be pointed out that vehicle exhausts and roadside vegetation are important sources for VOCs and NO_x in this road environment. However, the number of unique CHON_1 and CHON_2 compounds identified in the comparative cases with-

out water spray treatment was much less than that identified in the comparative cases with air spraying and ground aspersion treatments (Figs. 6 and S6). In particular, we did not observe significant oligomerization of CHON compounds after air spraying (Fig. S7). Thus, these results suggested that the increase in ALW caused by air spraying can facilitate the formation of organic nitrates via CHO compounds as potential precursors under the presence of NO_x .

3.4 Environmental implication

Mist cannon sprayers are commonly applied in agriculture for the distribution of fertilizers, pesticides and herbicides. In recent years, misting cannon trucks are widely developed and regarded as an excellent option for road dust control due to the production of tiny water droplets that can drop dust to the ground. In particular, it was a high-performance system for spraying disinfectant in the road environment during the COVID-19 epidemic period. For the first time, we provide a detailed characterization of chemical compositions in road-derived $\text{PM}_{2.5}$ under the influence of air spraying. A recent study conducted in a rural site (Shanghai, China) has suggested that gaseous water-soluble organic compounds mainly partitioned to the organic phase (organic shell) under the condition of RH less than 80% (relatively low ALW) but to ALW under the humid condition ($\text{RH} > 80\%$, as air spray-

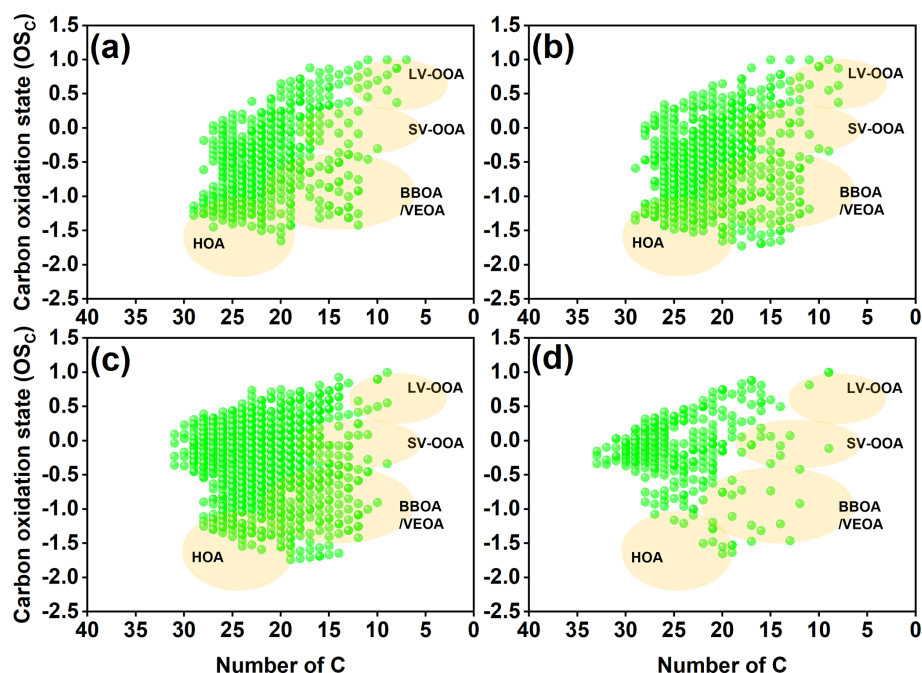


Figure 5. OS_C of unique CHO molecules in WSOM in $PM_{2.5}$ collected from different cases: air spray vs. ground aspersion on (a) 23 March, (b) 24 March and (c) 25 March and two road segments without water spray (I vs. II) on (d) 26 March. For the above comparative cases, the unique CHO compounds indicate the CHO molecules identified in $PM_{2.5}$ collected from the air spray (or no water spray, I) road segments. The light-orange background represents areas of HOA (hydrocarbon-like organic aerosol), BBOAs and VEOAs (biomass burning and vehicle emission organic aerosols; Kroll et al., 2011; Tong et al., 2016), SV-OOA (semivolatile oxidized organic aerosol), and LV-OOA (low-volatility oxidized organic aerosol; Kroll et al., 2011).

ing operation), highlighting the importance of high ALW in SOA formation processes (Lv et al., 2022). This is because aerosols can exist in a phase-separated form with an inorganic core and an organic shell (Yu et al., 2019; W. Li et al., 2021; Ushijima et al., 2021). Our results verified the formation of numerous unique CHO and CHON compounds by ALW-related promoting effects (Fig. 7). In particular, the mass concentrations of WSOC in $PM_{2.5}$ increased by 62%–70% after air spraying. Clearly, although the air spraying by mist cannon system could exert a better effect on suppressing road dust than the ground aspersion, as discussed previously, air pollution induced by increased water-soluble organic compounds in $PM_{2.5}$ will be exacerbated in the road environment.

To reveal the influence of air spraying on $PM_{2.5}$ pollution on the roadside, we investigated the time series of percentage variation in road $PM_{2.5}$ mass concentration after the mist cannon truck was operated at a low speed ($< 30 \text{ km h}^{-1}$) (Fig. 8). It should be pointed out that the mist cannon truck was usually operated back and forth on specific road sections to prevent the resuspension of dust. After the misting cannon truck passed through the monitoring site several times, repeated online $PM_{2.5}$ monitoring ($n = 34$, within a month) was performed to exclude the impact of dispersion and traffic flow on analysis results. Accordingly, the resuspension

of road dust was expected to exert a relatively minor impact on the $PM_{2.5}$ level near the road. The concentration of $PM_{2.5}$ showed an increasing trend after the mist cannon truck passed through the monitoring point for 15 min. Thus, the water droplets sprayed by the mist cannon truck cannot directly cause an increase in $PM_{2.5}$ concentration, suggesting that the increased $PM_{2.5}$ should be secondarily formed after water mist spraying ($\sim 15 \text{ min}$). This consideration was also supported by a significant increase in the concentration and number of water-soluble organic compounds after air spraying (Figs. 2 and 3). After the mist cannon truck has passed for 25–35 min, the increased proportion of $PM_{2.5}$ concentration on the roadside gradually reached the maximum ($\sim 13 \%$, on average). Subsequently, the proportion of increase in $PM_{2.5}$ concentration gradually decreased, reaching $\sim 6 \%$ at 50 min after the mist cannon truck was operated. In addition, the width of the road segment (81 road, Nanchang, China) where $PM_{2.5}$ was monitored is very large ($\sim 43 \text{ m}$), implying that the water mist sprayed by mist cannon trucks should exert a greater promoting effect on the formation of $PM_{2.5}$ on conventional urban roads. The overall results suggested that mist cannon trucks cannot effectively reduce the $PM_{2.5}$ level in the road environment but lead to aggravation of $PM_{2.5}$ pollution.

The chemical composition of fine aerosol particles in the urban road atmosphere is highly complex, including a lot of

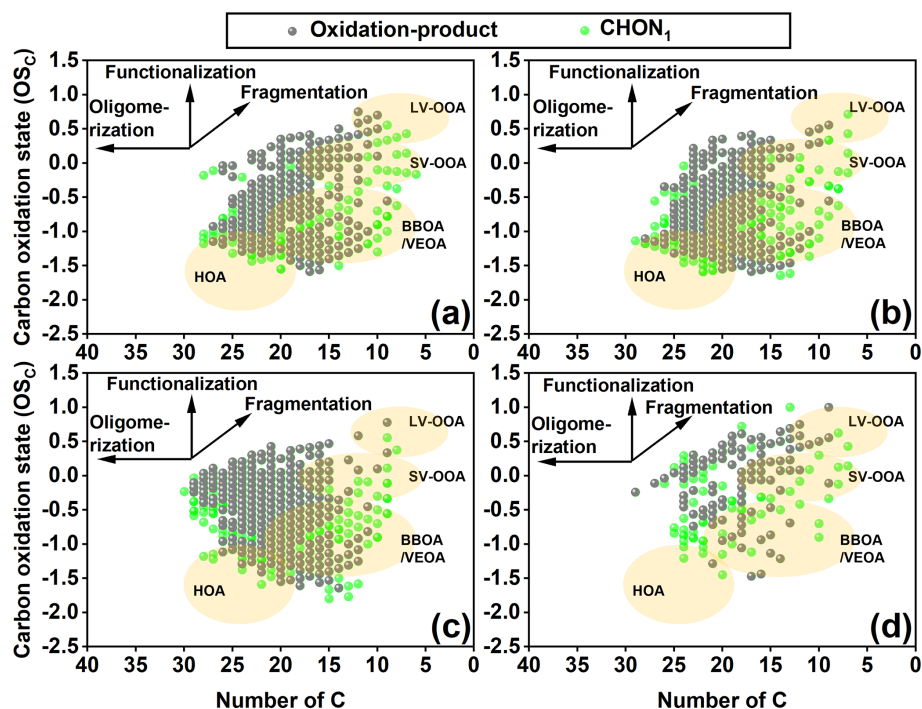


Figure 6. OS_C of unique $CHON_1$ molecules in WSOM in $PM_{2.5}$ collected from different cases: air spray vs. ground aspersion on (a) 23 March, (b) 24 March and (c) 25 March and two road segments without water spray (I vs. II) on (d) 26 March. For the above comparative cases, the unique $CHON_1$ compounds indicate the $CHON_1$ molecules identified in $PM_{2.5}$ collected from the air spray (or no water spray, I) road segments. The light-orange background represents areas of HOA, BBOA and VEOA, SV-OOA, and LV-OOA. The grey circles refer to the identified oxidation-product pairs.

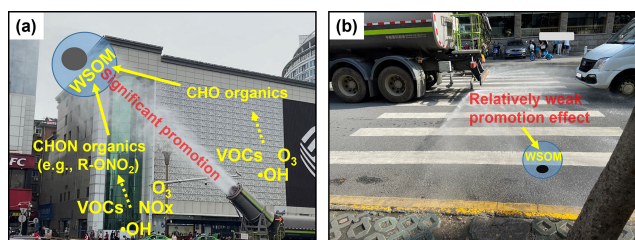


Figure 7. Conceptual picture showing the influence of (a) a mist cannon truck and (b) a traditional sprinkling truck on water-soluble organic matter (WSOM) formation in the urban road environment.

harmful organic compounds (e.g., polycyclic aromatic hydrocarbons and nitro-aromatics), as indicated by our measurements and a previous study (Tong et al., 2016). Emissions from vehicles and roadside vegetation are important anthropogenic and biogenic sources of reactive gas-phase OC and key precursors for forming SOA in urban areas (Gentner et al., 2012; Xu et al., 2020b; Tong et al., 2016). In particular, organic aerosol composition in the road environment can be strongly impacted by vehicle emissions (e.g., VOCs and NO_x) (Tong et al., 2016). Inhalation of the particles containing harmful organics can be responsible for a number of adverse health effects (Künzli et al., 2000). How-

ever, the wide application of mist cannon trucks by local environmental protection departments undoubtedly accelerates the formation processes of water-soluble organic compounds and $PM_{2.5}$, which will further worsen the urban road environment and cause health hazards to walking residents. Thus, the present study provides crucial information for the decision makers to regulate the mist cannon truck operation in many cities in China.

4 Conclusions

We investigated the changes in the chemical composition of $PM_{2.5}$ collected from the road sides of the urban road during the simulated operations of mist cannon trucks and traditional sprinkling trucks. Moreover, we also conducted online measurement of $PM_{2.5}$ concentration in the urban road segment where the mist cannon truck passed by. The mass concentrations of WSOC in $PM_{2.5}$ increased significantly (62%–70%) from the ground aspersion road segment to the air spray road segment. Similarly, ALW also showed a significant increase after air spraying. We found that the mass concentration of ALW in $PM_{2.5}$ was significantly positively correlated with that of WSOC and WSON. Thus, the increase of ALW after air spraying can promote the formation of particle-phase water-soluble organic compounds in

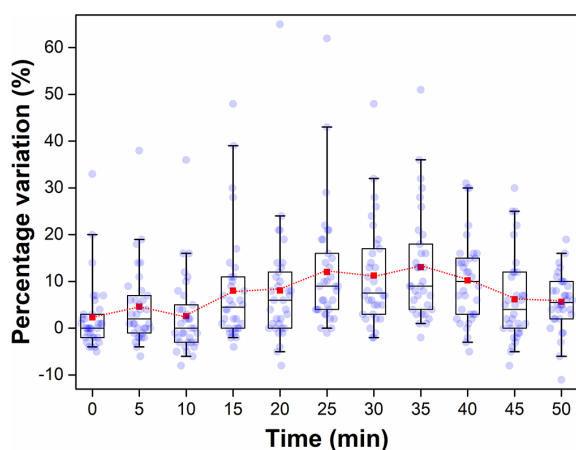


Figure 8. The time series of percentage variations in $\text{PM}_{2.5}$ mass concentrations after mist cannon truck operation ($n = 34$). Each box encompasses the 25th–75th percentiles. Whiskers are the 5th and 95th percentiles. The solid lines and squares inside boxes indicate the median and mean. All individual data are presented as circles.

the road environment. In addition, the decrease in Ca^{2+} and Mg^{2+} concentrations after air spraying suggested that the water mist sprayed by mist cannon trucks has a better effect on suppressing road dust than the ground aspersion by traditional sprinkling trucks.

A comparison in the number of CHO and CHON species between the air spraying and ground aspersion road segments suggested that the increase in ALW after air spraying can enhance the abundance and diversity of CHO and CHON compounds in $\text{PM}_{2.5}$. The unique CHO compounds formed after air spraying can be largely attributed to secondary processes associated with the oxidation of vehicle exhausts and biogenic VOCs by oxidants and the oligomerization of CHO compounds. Organic nitrates were considered to be the abundant nitrogen-containing compounds in $\text{PM}_{2.5}$. Furthermore, we found that the increased organic nitrates were largely derived from the transformation of CHO species under the existence of NO_x .

After the mist cannon truck has passed for 25–35 min, $\text{PM}_{2.5}$ concentration on the road side increased by up to 13 %, on average. The proportion of increase in $\text{PM}_{2.5}$ concentration gradually decreased to $\sim 6\%$ at 50 min after the mist cannon truck was operated. The overall results suggested that although mist cannon trucks could suppress road dust better than the traditional sprinkling truck, air pollution induced by increased aerosol water-soluble organic compounds and $\text{PM}_{2.5}$ levels will be exacerbated in the urban road environment. Our findings provide new insights into the formation processes of aerosol water-soluble organic compounds associated with the water mist sprayed by mist cannon trucks in the road atmospheric environment.

Data availability. The data presented in this work are available upon request from the corresponding authors.

Supplement. The supplement related to this article is available online at: <https://doi.org/10.5194/acp-23-6775-2023-supplement>.

Author contributions. YX, HYX and DW designed the study; YX, XD and HWX performed the field measurements; YX and CH performed the chemical analysis and data analysis; YX wrote the original paper; and YX reviewed and edited the paper.

Competing interests. The contact author has declared that none of the authors has any competing interests.

Disclaimer. Publisher's note: Copernicus Publications remains neutral with regard to jurisdictional claims in published maps and institutional affiliations.

Acknowledgements. The authors are very grateful to Chen-Xi Li for his kind and valuable comments to improve the paper.

Financial support. This research has been supported by the Shanghai Sailing Program (grant no. 22YF1418700) and the Natural (Youth) Science Foundation of Jiangxi, China (grant no. 20212BAB213039).

Review statement. This paper was edited by Annele Virtanen and reviewed by two anonymous referees.

References

- Aiken, A. C., DeCarlo, P. F., Kroll, J. H., Worsnop, D. R., Huffman, J. A., Docherty, K. S., Ulbrich, I. M., Mohr, C., Kimmel, J. R., Sueper, D., Sun, Y., Zhang, Q., Trimborn, A., Northway, M., Ziemann, P. J., Canagaratna, M. R., Onasch, T. B., Alfarra, M. R., Prevot, A. S. H., Dommen, J., Duplissy, J., Metzger, A., Baltensperger, U., and Jimenez, J. L.: O/C and OM/OC Ratios of Primary, Secondary, and Ambient Organic Aerosols with High-Resolution Time-of-Flight Aerosol Mass Spectrometry, *Environ. Sci. Technol.*, 42, 4478–4485, <https://doi.org/10.1021/es703009q>, 2008.
- Altieri, K. E., Turpin, B. J., and Seitzinger, S. P.: Oligomers, organosulfates, and nitrooxy organosulfates in rainwater identified by ultra-high resolution electrospray ionization FT-ICR mass spectrometry, *Atmos. Chem. Phys.*, 9, 2533–2542, <https://doi.org/10.5194/acp-9-2533-2009>, 2009.
- Bean, J. K. and Hildebrandt Ruiz, L.: Gas-particle partitioning and hydrolysis of organic nitrates formed from the oxidation of α -pinene in environmental chamber experiments, *At-*

- mos. Chem. Phys., 16, 2175–2184, <https://doi.org/10.5194/acp-16-2175-2016>, 2016.
- Carlton, A. G. and Turpin, B. J.: Particle partitioning potential of organic compounds is highest in the Eastern US and driven by anthropogenic water, *Atmos. Chem. Phys.*, 13, 10203–10214, <https://doi.org/10.5194/acp-13-10203-2013>, 2013.
- Chen, H. Y. and Chen, L. D.: Importance of anthropogenic inputs and continental-derived dust for the distribution and flux of water-soluble nitrogen and phosphorus species in aerosol within the atmosphere over the East China Sea, *J. Geophys. Res.-Atmos.*, 113, D11303, <https://doi.org/10.1029/2007JD009491>, 2008.
- Chen, X., Wang, H., Lu, K., Li, C., Zhai, T., Tan, Z., Ma, X., Yang, X., Liu, Y., Chen, S., Dong, H., Li, X., Wu, Z., Hu, M., Zeng, L., and Zhang, Y.: Field Determination of Nitrate Formation Pathway in Winter Beijing, *Environ. Sci. Technol.*, 54, 9243–9253, <https://doi.org/10.1021/acs.est.0c00972>, 2020.
- Chen, Y., Wang, Y., Nenes, A., Wild, O., Song, S., Hu, D., Liu, D., He, J., Hildebrandt Ruiz, L., Apte, J. S., Gunthe, S. S., and Liu, P.: Ammonium Chloride Associated Aerosol Liquid Water Enhances Haze in Delhi, India, *Environ. Sci. Technol.*, 56, 7163–7173, <https://doi.org/10.1021/acs.est.2c00650>, 2022.
- Cruz, C. N. and Pandis, S. N.: Deliquescence and hygroscopic growth of mixed inorganic-organic atmospheric aerosol, *Environ. Sci. Technol.*, 34, 4313–4319, <https://doi.org/10.1021/es9907109>, 2000.
- Deng, F., Lv, Z., Qi, L., Wang, X., Shi, M., and Liu, H.: A big data approach to improving the vehicle emission inventory in China, *Nat. Commun.*, 11, 2801, <https://doi.org/10.1038/s41467-020-16579-w>, 2020.
- Dittmar, T., Koch, B., Hertkorn, N., and Kattner, G.: A simple and efficient method for the solid-phase extraction of dissolved organic matter (SPE-DOM) from seawater, *Limnol. Oceanogr.-Meth.*, 6, 230–235, 2008.
- Finessi, E., Decesari, S., Paglione, M., Giulianelli, L., Carbone, C., Gilardoni, S., Fuzzi, S., Saarikoski, S., Raatikainen, T., Hillamo, R., Allan, J., Mentel, Th. F., Tiitta, P., Laaksonen, A., Petäjä, T., Kulmala, M., Worsnop, D. R., and Facchini, M. C.: Determination of the biogenic secondary organic aerosol fraction in the boreal forest by NMR spectroscopy, *Atmos. Chem. Phys.*, 12, 941–959, <https://doi.org/10.5194/acp-12-941-2012>, 2012.
- Fu, X., Wang, T., Gao, J., Wang, P., Liu, Y., Wang, S., Zhao, B., and Xue, L.: Persistent Heavy Winter Nitrate Pollution Driven by Increased Photochemical Oxidants in Northern China, *Environ. Sci. Technol.*, 54, 3881–3889, <https://doi.org/10.1021/acs.est.9b07248>, 2020.
- Gentner, D. R., Isaacman, G., Worton, D. R., Chan, A. W. H., Dallmann, T. R., Davis, L., Liu, S., Day, D. A., Russell, L. M., Wilson, K. R., Weber, R., Guha, A., Harley, R. A., and Goldstein, A. H.: Elucidating secondary organic aerosol from diesel and gasoline vehicles through detailed characterization of organic carbon emissions, *P. Natl. Acad. Sci. USA*, 109, 18318–18323, <https://doi.org/10.1073/pnas.1212272109>, 2012.
- Guo, H., Xu, L., Bougiatioti, A., Cerully, K. M., Capps, S. L., Hite Jr., J. R., Carlton, A. G., Lee, S.-H., Bergin, M. H., Ng, N. L., Nenes, A., and Weber, R. J.: Fine-particle water and pH in the southeastern United States, *Atmos. Chem. Phys.*, 15, 5211–5228, <https://doi.org/10.5194/acp-15-5211-2015>, 2015.
- Hallquist, M., Wenger, J. C., Baltensperger, U., Rudich, Y., Simpson, D., Claeys, M., Dommen, J., Donahue, N. M., George, C., Goldstein, A. H., Hamilton, J. F., Herrmann, H., Hoffmann, T., Iinuma, Y., Jang, M., Jenkin, M. E., Jimenez, J. L., Kiendler-Scharr, A., Maenhaut, W., McFiggans, G., Mentel, Th. F., Monod, A., Prévôt, A. S. H., Seinfeld, J. H., Surratt, J. D., Szmigielski, R., and Wildt, J.: The formation, properties and impact of secondary organic aerosol: current and emerging issues, *Atmos. Chem. Phys.*, 9, 5155–5236, <https://doi.org/10.5194/acp-9-5155-2009>, 2009.
- He, C., Pan, Q., Li, P., Xie, W., He, D., Zhang, C., and Shi, Q.: Molecular composition and spatial distribution of dissolved organic matter (DOM) in the Pearl River Estuary, China, *Environ. Chem.*, 17, 240–251, <https://doi.org/10.1071/EN19051>, 2019.
- He, C., Zhang, Y., Li, Y., Zhuo, X., Li, Y., Zhang, C., and Shi, Q.: In-House Standard Method for Molecular Characterization of Dissolved Organic Matter by FT-ICR Mass Spectrometry, *ACS Omega*, 5, 11730–11736, <https://doi.org/10.1021/acsomega.0c01055>, 2020.
- Hodas, N., Sullivan, A. P., Skog, K., Keutsch, F. N., Collett Jr, J. L., Decesari, S., Facchini, M. C., Carlton, A. G., Laaksonen, A., and Turpin, B. J.: Aerosol liquid water driven by anthropogenic nitrate: Implications for lifetimes of water-soluble organic gases and potential for secondary organic aerosol formation, *Environ. Sci. Technol.*, 48, 11127–11136, <https://doi.org/10.1021/es5025096>, 2014.
- Hu, W., Hu, M., Hu, W.-W., Zheng, J., Chen, C., Wu, Y., and Guo, S.: Seasonal variations in high time-resolved chemical compositions, sources, and evolution of atmospheric submicron aerosols in the megacity Beijing, *Atmos. Chem. Phys.*, 17, 9979–10000, <https://doi.org/10.5194/acp-17-9979-2017>, 2017.
- Koch, B. P. and Dittmar, T.: From mass to structure: an aromaticity index for high-resolution mass data of natural organic matter, *Rapid Commun. Mass Sp.*, 20, 926–932, <https://doi.org/10.1002/rcm.2386>, 2006.
- Kroll, J. H., Donahue, N. M., Jimenez, J. L., Kessler, S. H., Canagaratna, M. R., Wilson, K. R., Altieri, K. E., Mazzoleni, L. R., Wozniak, A. S., Bluhm, H., Mysak, E. R., Smith, J. D., Kolb, C. E., and Worsnop, D. R.: Carbon oxidation state as a metric for describing the chemistry of atmospheric organic aerosol, *Nat. Chem.*, 3, 133–139, <https://doi.org/10.1038/nchem.948>, 2011.
- Künzli, N., Kaiser, R., Medina, S., Studnicka, M., Chanel, O., Filliger, P., Herry, M., Horak, F., Jr., Puybonnieux-Textier, V., Quénel, P., Schneider, J., Seethaler, R., Vergnaud, J. C., and Sommer, H.: Public-health impact of outdoor and traffic-related air pollution: a European assessment, *Lancet*, 356, 795–801, [https://doi.org/10.1016/S0140-6736\(00\)02653-2](https://doi.org/10.1016/S0140-6736(00)02653-2), 2000.
- Lee, B. H., Mohr, C., Lopez-Hilfiker, F. D., Lutz, A., Hallquist, M., Lee, L., Romer, P., Cohen, R. C., Iyer, S., Kurtén, T., Hu, W., Day, D. A., Campuzano-Jost, P., Jimenez, J. L., Xu, L., Ng, N. L., Guo, H., Weber, R. J., Wild, R. J., Brown, S. S., Koss, A., Gouw, J. d., Olson, K., Goldstein, A. H., Seco, R., Kim, S., McAvey, K., Shepson, P. B., Starn, T., Baumann, K., Edgerton, E. S., Liu, J., Shilling, J. E., Miller, D. O., Brune, W., Schobesberger, S., D'Ambro, E. L., and Thornton, J. A.: Highly functionalized organic nitrates in the southeast United States: Contribution to secondary organic aerosol and reactive nitrogen budgets, *P. Natl. Acad. Sci. USA*, 113, 1516–1521, <https://doi.org/10.1073/pnas.1508108113>, 2016.

- Li, W., Teng, X., Chen, X., Liu, L., Xu, L., Zhang, J., Wang, Y., Zhang, Y., and Shi, Z.: Organic Coating Reduces Hygroscopic Growth of Phase-Separated Aerosol Particles, *Environ. Sci. Technol.*, 55, 16339–16346, <https://doi.org/10.1021/acs.est.1c05901>, 2021.
- Li, X., Song, S., Zhou, W., Hao, J., Worsnop, D. R., and Jiang, J.: Interactions between aerosol organic components and liquid water content during haze episodes in Beijing, *Atmos. Chem. Phys.*, 19, 12163–12174, <https://doi.org/10.5194/acp-19-12163-2019>, 2019.
- Li, X., Zhang, Y., Shi, L., Kawamura, K., Kunwar, B., Takami, A., Arakaki, T., and Lai, S.: Aerosol Proteinaceous Matter in Coastal Okinawa, Japan: Influence of Long-Range Transport and Photochemical Degradation, *Environ. Sci. Technol.*, 56, 5256–5265, <https://doi.org/10.1021/acs.est.1c08658>, 2022.
- Li, Y., Zhao, J., Wang, Y., Seinfeld, J. H., and Zhang, R.: Multigeneration Production of Secondary Organic Aerosol from Toluene Photooxidation, *Environ. Sci. Technol.*, 55, 8592–8603, <https://doi.org/10.1021/acs.est.1c02026>, 2021.
- Lin, P., Liu, J., Shilling, J. E., Kathmann, S. M., Laskin, J., and Laskin, A.: Molecular characterization of brown carbon (BrC) chromophores in secondary organic aerosol generated from photo-oxidation of toluene, *Phys. Chem. Chem. Phys.*, 17, 23312–23325, <https://doi.org/10.1039/C5CP02563J>, 2015.
- Lv, S., Wang, F., Wu, C., Chen, Y., Liu, S., Zhang, S., Li, D., Du, W., Zhang, F., Wang, H., Huang, C., Fu, Q., Duan, Y., and Wang, G.: Gas-to-Aerosol Phase Partitioning of Atmospheric Water-Soluble Organic Compounds at a Rural Site in China: An Enhancing Effect of NH₃ on SOA Formation, *Environ. Sci. Technol.*, 56, 3915–3924, <https://doi.org/10.1021/acs.est.1c06855>, 2022.
- Ma, W., Zheng, F., Zhang, Y., Chen, X., Zhan, J., Hua, C., Song, B., Wang, Z., Xie, J., Yan, C., Kulmala, M., and Liu, Y.: Weakened Gas-to-Particle Partitioning of Oxygenated Organic Molecules in Liquefied Aerosol Particles, *Environ. Sci. Technol.*, 9, 837–843, <https://doi.org/10.1021/acs.estlett.2c00556>, 2022.
- Mozurkewich, M.: The dissociation constant of ammonium nitrate and its dependence on temperature, relative humidity and particle size, *Atmos. Environ.*, 27, 261–270, [https://doi.org/10.1016/0960-1686\(93\)90356-4](https://doi.org/10.1016/0960-1686(93)90356-4), 1993.
- Müller, A., Miyazaki, Y., Tachibana, E., Kawamura, K., and Hiura, T.: Evidence of a reduction in cloud condensation nuclei activity of water-soluble aerosols caused by biogenic emissions in a cool-temperate forest, *Sci. Rep.*, 7, 8452, <https://doi.org/10.1038/s41598-017-08112-9>, 2017.
- Nguyen, T. K. V., Capps, S. L., and Carlton, A. G.: Decreasing Aerosol Water Is Consistent with OC Trends in the Southeast U.S., *Environ. Sci. Technol.*, 49, 7843–7850, <https://doi.org/10.1021/acs.est.5b00828>, 2015.
- Nguyen, T. K. V., Zhang, Q., Jimenez, J. L., Pike, M., and Carlton, A. G.: Liquid water: ubiquitous contributor to aerosol mass, *Environ. Sci. Technol.*, 3, 257–263, <https://doi.org/10.1021/acs.estlett.6b00167>, 2016.
- Qiao, W., Guo, H., He, C., Shi, Q., Xiu, W., and Zhao, B.: Molecular Evidence of Arsenic Mobility Linked to Biodegradable Organic Matter, *Environ. Sci. Technol.*, 54, 7280–7290, <https://doi.org/10.1021/acs.est.0c00737>, 2020.
- Qiu, Y., Xie, Q., Wang, J., Xu, W., Li, L., Wang, Q., Zhao, J., Chen, Y., Chen, Y., Wu, Y., Du, W., Zhou, W., Lee, J., Zhao, C., Ge, X., Fu, P., Wang, Z., Worsnop, D. R., and Sun, Y.: Vertical Characterization and Source Apportionment of Water-Soluble Organic Aerosol with High-resolution Aerosol Mass Spectrometry in Beijing, China, *ACS Earth Space Chem.*, 3, 273–284, <https://doi.org/10.1021/acsearthspacechem.8b00155>, 2019.
- Sareen, N., Schwieter, A., Latham, T., Nenes, A., and McNeill, V. F.: Surfactants from the gas phase may promote cloud droplet formation, *P. Natl. Acad. Sci. USA*, 110, 2723–2728, <https://doi.org/10.1073/pnas.1204838110>, 2013.
- Sareen, N., Waxman, E. M., Turpin, B. J., Volkamer, R., and Carlton, A. G.: Potential of aerosol liquid water to facilitate organic aerosol formation: assessing knowledge gaps about precursors and partitioning, *Environ. Sci. Technol.*, 51, 3327–3335, 2017.
- Schmidt, F., Koch, B. P., Goldhammer, T., Elvert, M., Witt, M., Lin, Y.-S., Wendt, J., Zabel, M., Heuer, V. B., and Hinrichs, K.-U.: Unraveling signatures of biogeochemical processes and the depositional setting in the molecular composition of pore water DOM across different marine environments, *Geochim. Cosmochim. Ac.*, 207, 57–80, <https://doi.org/10.1016/j.gca.2017.03.005>, 2017.
- Simon, H., Bhavsar, P. V., Swall, J. L., Frank, N. H., and Malm, W. C.: Determining the spatial and seasonal variability in OM/OC ratios across the US using multiple regression, *Atmos. Chem. Phys.*, 11, 2933–2949, <https://doi.org/10.5194/acp-11-2933-2011>, 2011.
- Song, J., Li, M., Jiang, B., Wei, S., Fan, X., and Peng, P. A.: Molecular Characterization of Water-Soluble Humic like Substances in Smoke Particles Emitted from Combustion of Biomass Materials and Coal Using Ultrahigh-Resolution Electrospray Ionization Fourier Transform Ion Cyclotron Resonance Mass Spectrometry, *Environ. Sci. Technol.*, 52, 2575–2585, <https://doi.org/10.1021/acs.est.7b06126>, 2018.
- Su, S., Xie, Q., Lang, Y., Cao, D., Xu, Y., Chen, J., Chen, S., Hu, W., Qi, Y., Pan, X., Sun, Y., Wang, Z., Liu, C.-Q., Jiang, G., and Fu, P.: High Molecular Diversity of Organic Nitrogen in Urban Snow in North China, *Environ. Sci. Technol.*, 55, 4344–4356, <https://doi.org/10.1021/acs.est.0c06851>, 2021.
- Sun, Y., Du, W., Fu, P., Wang, Q., Li, J., Ge, X., Zhang, Q., Zhu, C., Ren, L., Xu, W., Zhao, J., Han, T., Worsnop, D. R., and Wang, Z.: Primary and secondary aerosols in Beijing in winter: sources, variations and processes, *Atmos. Chem. Phys.*, 16, 8309–8329, <https://doi.org/10.5194/acp-16-8309-2016>, 2016.
- Tan, H., Cai, M., Fan, Q., Liu, L., Li, F., Chan, P. W., Deng, X., and Wu, D.: An analysis of aerosol liquid water content and related impact factors in Pearl River Delta, *Sci. Total Environ.*, 579, 1822–1830, <https://doi.org/10.1016/j.scitotenv.2016.11.167>, 2017.
- Tong, H., Kourtchev, I., Pant, P., Keyte, I., O'Connor, I. P., Wenger, J., Pope, F., Harrison, R., and Kalberer, M.: Molecular composition of organic aerosols at urban background and road tunnel sites using ultra-high resolution mass spectrometry, *Faraday Discuss.*, 189, 51–68, <https://doi.org/10.17863/CAM.5910>, 2016.
- Ushijima, S. B., Huynh, E., Davis, R. D., and Tolbert, M. A.: Seeded Crystal Growth of Internally Mixed Organic–Inorganic Aerosols: Impact of Organic Phase State, *J. Phys. Chem. A*, 125, 8668–8679, <https://doi.org/10.1021/acs.jpca.1c04471>, 2021.
- Wang, J., Ye, J., Zhang, Q., Zhao, J., Wu, Y., Li, J., Liu, D., Li, W., Zhang, Y., Wu, C., Xie, C., Qin, Y., Lei, Y., Huang, X., Guo, J., Liu, P., Fu, P., Li, Y., Lee, H. C., Choi, H., Zhang, J., Liao,

- H., Chen, M., Sun, Y., Ge, X., Martin, S. T., and Jacob, D. J.: Aqueous production of secondary organic aerosol from fossil-fuel emissions in winter Beijing haze, *P. Natl. Acad. Sci.*, 118, e2022179118, <https://doi.org/10.1073/pnas.2022179118>, 2021.
- Wang, J., Gui, H., Yang, Z., Yu, T., Zhang, X., and Liu, J.: Real-world gaseous emission characteristics of natural gas heavy-duty sanitation trucks, *J. Environ. Sci.*, 115, 319–329, <https://doi.org/10.1016/j.jes.2021.06.023>, 2022.
- Xie, Q., Su, S., Chen, S., Xu, Y., Cao, D., Chen, J., Ren, L., Yue, S., Zhao, W., Sun, Y., Wang, Z., Tong, H., Su, H., Cheng, Y., Kawamura, K., Jiang, G., Liu, C.-Q., and Fu, P.: Molecular characterization of firework-related urban aerosols using Fourier transform ion cyclotron resonance mass spectrometry, *Atmos. Chem. Phys.*, 20, 6803–6820, <https://doi.org/10.5194/acp-20-6803-2020>, 2020.
- Xu, Y., Wu, D. S., Xiao, H. Y., and Zhou, J. X.: Dissolved hydrolyzed amino acids in precipitation in suburban Guiyang, southwestern China: Seasonal variations and potential atmospheric processes, *Atmos. Environ.*, 211, 247–255, <https://doi.org/10.1016/j.atmosenv.2019.05.011>, 2019.
- Xu, Y., Xiao, H., Wu, D., and Long, C.: Abiotic and Biological Degradation of Atmospheric Proteinaceous Matter Can Contribute Significantly to Dissolved Amino Acids in Wet Deposition, *Environ. Sci. Technol.*, 54, 6551–6561, <https://doi.org/10.1021/acs.est.0c00421>, 2020a.
- Xu, Y., Miyazaki, Y., Tachibana, E., Sato, K., Ramasamy, S., Mochizuki, T., Sadanaga, Y., Nakashima, Y., Sakamoto, Y., Matsuda, K., and Kajii, Y.: Aerosol Liquid Water Promotes the Formation of Water-Soluble Organic Nitrogen in Submicrometer Aerosols in a Suburban Forest, *Environ. Sci. Technol.*, 54, 1406–1414, <https://doi.org/10.1021/acs.est.9b05849>, 2020b.
- Xu, Y., Dong, X.-N., Xiao, H.-Y., Zhou, J.-X., and Wu, D.-S.: Proteinaceous Matter and Liquid Water in Fine Aerosols in Nanchang, Eastern China: Seasonal Variations, Sources, and Potential Connections, *J. Geophys. Res.-Atmos.*, 127, e2022JD036589, <https://doi.org/10.1029/2022JD036589>, 2022.
- Yang, D., Zhu, S., Ma, Y., Zhou, L., Zheng, F., Wang, L., Jiang, J., and Zheng, J.: Emissions of Ammonia and Other Nitrogen-Containing Volatile Organic Compounds from Motor Vehicles under Low-Speed Driving Conditions, *Environ. Sci. Technol.*, 56, 5440–5447, <https://doi.org/10.1021/acs.est.2c00555>, 2022.
- Yeh, G. K. and Ziemann, P. J.: Alkyl Nitrate Formation from the Reactions of C8–C14 n-Alkanes with OH Radicals in the Presence of NOx: Measured Yields with Essential Corrections for Gas–Wall Partitioning, *J. Phys. Chem. A*, 118, 8147–8157, <https://doi.org/10.1021/jp500631v>, 2014.
- Yttri, K. E., Aas, W., Bjerke, A., Cape, J. N., Cavalli, F., Ceburnis, D., Dye, C., Emblico, L., Facchini, M. C., Forster, C., Hanssen, J. E., Hansson, H. C., Jennings, S. G., Maenhaut, W., Putaud, J. P., and Tørseth, K.: Elemental and organic carbon in PM₁₀: a one year measurement campaign within the European Monitoring and Evaluation Programme EMEP, *Atmos. Chem. Phys.*, 7, 5711–5725, <https://doi.org/10.5194/acp-7-5711-2007>, 2007.
- Yu, H., Li, W., Zhang, Y., Tunved, P., Dall’Osto, M., Shen, X., Sun, J., Zhang, X., Zhang, J., and Shi, Z.: Organic coating on sulfate and soot particles during late summer in the Svalbard Archipelago, *Atmos. Chem. Phys.*, 19, 10433–10446, <https://doi.org/10.5194/acp-19-10433-2019>, 2019.
- Yue, H., He, C., Huang, Q., Yin, D., and Bryan, B. A.: Stronger policy required to substantially reduce deaths from PM_{2.5} pollution in China, *Nat. Commun.*, 11, 1462, <https://doi.org/10.1038/s41467-020-15319-4>, 2020.